ELSEVIER

Polymer 43 (2002) 6123–6130

polymer

www.elsevier.com/locate/polymer

Excimers in dilute solutions of *N*-vinyl carbazole/styrene copolymers of different molar compositions

Alejandro Sanz, Francisco Mendicuti*

Departamento de Química Física, Universidad de Alcalá, 28871 Alcalá de Henares, Madrid, Spain

Received 2 October 2001; accepted 13 August 2002

Abstract

Steady-state fluorescence for dilute solutions of poly(*N*-vinyl carbazole) and *N*-vinyl carbazole/styrene copolymers of different molar monomer compositions upon excitation of carbazole groups were performed. I_E/I_M ratios depend on solvent nature, emission wavelength and copolymer composition. Molecular dynamics simulations on pure isotactic and sindiotactic fragments of different monomer compositions were used for identifying the amount and the conformations capable of forming intramolecular excimers. The analysis of theoretical results interprets the variation of the amount of intramolecular excimer with the molar monomer content. Types of complexes by total or partial overlapping between adjacent and non-adjacent carbazole chromophores were also distinguished.

Keywords: Excimer; Poly(*N*-vinyl carbazole); Copolymers

1. Introduction

The photophysics of poly(*N*-vinyl carbazole), PVCz, have been extensively studied both in solution and solid state [1]. Its photoconductive properties and its distinctive excimer-forming characteristics are some of the reasons for such interest. Emission spectrum of PVCz consists of the monomer and two excimer emission bands, centered at ~370 and ~420 nm. These excimers, named high- and low-energy excimers, respectively, seem to arise from those conformations, where rings of two carbazole groups partially and totally overlap. To contribute to the understanding of the structural origin of such excimers, as well as their mechanism of formation, much work, mostly experimental, has been done on PVCz [2–7], dimeric PVCz model compounds [8–17] and VCz-containing copolymers [6,18–21]. However, given the conformational dependence of intramolecular excimers, theoretical treatments of the accessible conformations, at the equilibrium [22] or by molecular dynamics simulations [23], are useful to strengthen the understanding of this phenomenon.

In this sense we have recently reported [21] an experimental and theoretical study on the intramolecular excimer formation on PVCz and *N*-vinyl carbazole/MMA copolymers of different molar compositions. The experimental part was performed in dilute solution of several solvents including a rigid solid matrix of PMMA. Molecular dynamics (MD) simulations were performed on pure iso- and sindiotactic forms of $CH_3-A-CH_2-B_n-A-CH_2-B_n-A-CH_3$ trichromophoric fragments ($n = 0–5$), where A = –CHCz–, B = $-C(CH_3)COOCH_3-CH_2-$, and on *meso*- and *racemic* forms of the 2,4-di(*N*-carbazolyl)pentane. Results permit us to state, among others, the following facts: (a) the amount of intramolecular excimers in the copolymers decreases as the molar Cz content decreases, this trend is also observed in the MD simulations; (b) excimers seem to be mostly populated by interaction between Cz groups from the Cz–Cz sequences of the polymer chain, which is also corroborated in the MD; (c) MD suggests that excimer formation is more likely in isotactic fragments than in syndiotactic ones and (d) MD also shows that the low-energy excimer conformations have higher probability for isotactic chains than for syndiotactic ones.

Here we carry out a similar study of the intramolecular excimer formation in dilute solutions of VCz/styrene copolymers of different molar compositions upon excitation of Cz groups. We also use MD on isotactic and sindiotactic fragments containing three carbazole groups represented by

* Corresponding author. Tel.: +34-91-8854672; fax: +34-91-8854763.
E-mail address: francisco.mendicuti@uah.es (F. Mendicuti).

0032-3861/02/$ - see front matter
PII: S0032-3861(02)00584-0

$CH_3-A-CH_2-B_n-A-CH_2-B_n-A-CH_3$ ($n = 0-5$), where A = –CHCz–, B = –CHBz–CH_2– and Bz = benzyl group, to rationalize the experimental results.

2. Experimental part

2.1. Materials and methods

Commercial 2,2′-azobis(2-metilpropionitrilo) (AIBN, Acros 98%) was used as purchased. Commercially available *N*-vinyl carbazole (VCz, Aldrich 98%) was purified by recrystallization (× 2) from methanol. Commercial styrene, stabilized with 4-*tert*-butylpyrocathecol (ST, Merck, 99%) was distilled under vacuum to remove the inhibitor. Ethylcarbazole, commercially available (ECz, Aldrich, 98%) and ethylbenzene (EBz, Fluka, >99%) were used as model compounds. ECz was purified by recrystallization (× 2) from methanol and EBz was used as received. Polystyrene (PS, Aldrich, MW = 32 600) used in some measurements was commercial. MMA stabilized with methylhidroquinone (MMA, Acros) was distilled under vacuum to remove the inhibitor. Solvents benzene, *p*-dioxane, tetrahydrofurane and methanol (Panreac, reagent grade) and petroleum ether (Scharlau, reagent grade) were used either for synthesis or as precipitant agents. Solvents used in spectroscopic measurements, *p*-dioxane (*p*-D), 1,2-dichloroethane (DCE), dichloromethane (DCM), methanol (MET), and tetrahydrofurane (THF), (Aldrich, spectrophotometric grade) were checked by fluorescence before using and they were used without further purification.

2.2. Preparation, purification and characterization

Synthesis of homopolymer, poly(*N*-vinyl carbazole), PVCz and copolymers of *N*-vinyl carbazole /styrene with different molar monomer compositions, whose structure is depicted in Fig. 1, were carried out by free radical polymerization in the presence of an initiator (AIBN, 1 mg per gram of initial reactive mixture) under different experimental conditions. For simplicity, polymers were named sequentially from P0 (PVCz) to P10 (PS), where the digit increases from 1 to 9 as the ST monomer content in feed mixture increases.

PVCz homopolymer, P0. The mixture of VCz and AIBN in the absence of any solvent was heated at 75 °C in a test tube for 5 h. Before the reaction, nitrogen was bubbled through it for 15 min and then the reaction tube was kept under nitrogen atmosphere. Once the reaction was stopped, by placing the reaction tube in an ice bath, the content was dissolved in tetrahydrofurane and precipitated with cold methanol. Similar experimental conditions for the mixture of VCz and ST monomers, but with a reaction time of ~3 h 45 min, were used for P2, P3, P4 and P5. Initial reaction mixtures of VCz and ST were, respectively, 6.0, 3.5; 5.6, 4.0; 4.5, 6.1 and 3.8 mmol, 6.9 mmol. Something similar

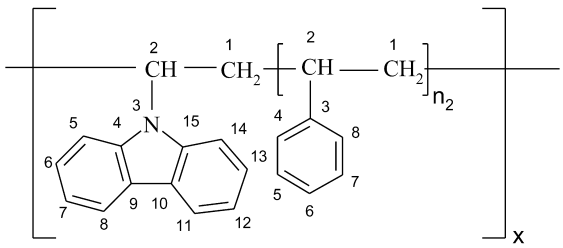

Fig. 1. Labeled structure of poly(VCz-*co*-ST) copolymers.

occurs with P6 and P9, but the reactions were carried out for 1 h 30 min at 70 °C. In this occasion the initial reacting mixture content of VCz and ST monomers were, respectively, 2.12, 6.1 and 0.52 mmol, 9.6 mmol.

Copolymers named P1, P7 and P8 were prepared by using benzene as a solvent. The cold benzene solution mixture of VCz and ST, containing the appropriate amount of AIBN, was deoxygenated by bubbling with nitrogen for about 15 min. VCz and ST content in the feeding mixture were, respectively, 2.7, 0.14; 0.88, 3.62 and 1.2 mmol, 10.8 mmol for P1, P7 and P8. Then the mixture was heated under nitrogen at 70 °C during approximately 10 h. Termination was achieved by placing the reaction tube in an ice bath. The content of the tube was poured in cold methanol.

After precipitation of any of the samples, regardless of the method used, a solid white product, whose external appearance before filtering depends on feeding monomer compositions is obtained. Stickiness increases as the ST content increases. The polymer samples were isolated by filtration and dried in the vacuum oven at a temperature of ~35 °C.

NMR and mainly GPC reveals the presence in the products of a significant amount of unreacted VCz monomer. A first step in a further purification procedure involves washing the products with petroleum ether (VCz is almost soluble) several times. Once filtered, the solid product is purified by reprecipitation (× 2) from *p*-dioxane into petroleum ether in an ice bath, keeping the solution cold for 20 h. Then the samples were filtered and dried in a vacuum oven at ~35 °C. Purity was checked by UV/vis, GPC and NMR.

Composition of the copolymers was determined by elemental analysis of the nitrogen, carbon and hydrogen percent content. Elemental analysis gave: P1 (N = 6.26, C = 84.83, H = 6.50); P2 (N = 1.45, C = 90.48, H = 7.47); P3 (N = 1.32, C = 90.05, H = 7.27); P4 (N = 1.23, C = 91.41, H = 7.60); P5 (N = 0.78, C = 89.41, H = 7.42); P6 (N = 0.27, C = 91.12, H = 7.47); P7 (N = 0.62, C = 90.31, H = 8.14); P8 (N = 0.26, C = 90.85, H = 8.21); P9 (N = 0.38, C = 91.61, H = 7.58). The reactivity ratios of VCz (r_1) and ST (r_2) monomers were obtained by the methods of Fineman–Ross [24] and Kelen–Tüdos [25]. Both methods gave very similar values of $r_1 = 0.11 \pm 0.30$; $r_2 = 5.27 \pm 0.43$ and $r_1 = 0.12 \pm 0.12$; $r_2 = 4.82 \pm 0.70$, respectively. The

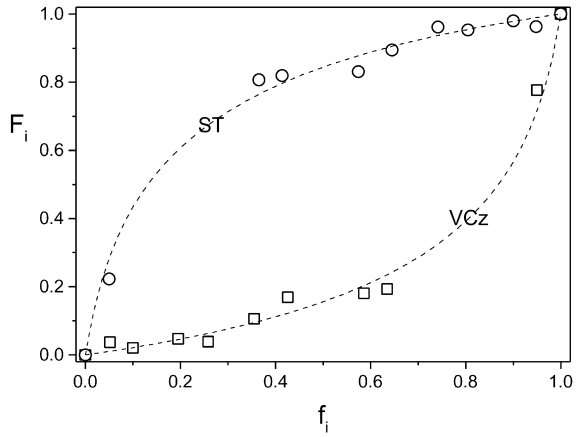

Fig. 2. Composition diagram for *N*-vinyl carbazole /styrene copolymerization: f_i mol fraction of monomer in feed; F_i mole fraction of monomers in copolymer. Fitting curves are obtained by using as monomer reactivity ratios an average of the values obtained by Fineman–Ross [24] and Kelen–Tüdos [25] methods.

dependence of the copolymer composition on the comonomer, VCz and ST, feed composition and fitting curve taking into account the average of these parameters $\bar{r}_i$, is reported in Fig. 2. Table 1 collects the initial and final composition of the copolymers, and the number average sequence length of the VCz ($\bar{n}_1$) and the ST ($\bar{n}_2$) monomer units defined as

$$\bar{n}_1 = \frac{\bar{r}_1 f_1 + f_2}{f_2} \quad \text{and} \quad \bar{n}_2 = \frac{\bar{r}_2 f_2 + f_1}{f_1}. \tag{1}$$

2.3. Spectroscopic measurements

Fig. 3 depicts absorption spectra (Hewlett Packard 8452A Dyode Array Spectrophotometer) for ECz, EBz and copolymer P3 in *p*-dioxane at 25 °C. In general, all copolymers P1–P9 show similar spectra, with bands that result from a combination of spectra of ECz and EBz. They

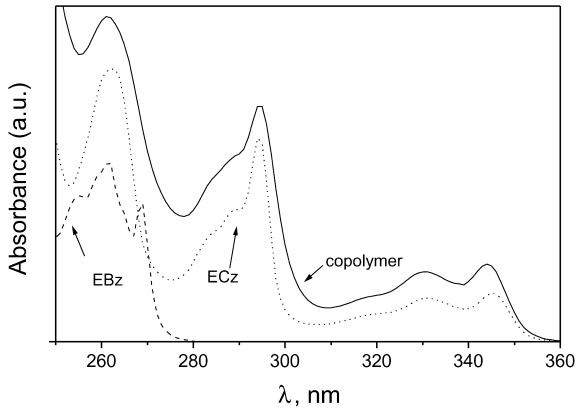

Fig. 3. Absorption spectra for ECz, EBz and copolymer P3 in *p*-dioxane at 25 °C.

present distinguishable bands centered around 265, 295, 331 and 345 nm. Similar spectra were obtained in other solvents. Spectra for homopolymers, P0 and PS, look like those for their ECz and EBz models, respectively. Changing the copolymer composition does not result in a substantial modification of the spectra bands placement.

Fluorescence measurements were performed using an SLM 8100 Aminco whose characteristics were reported previously [21]. Excitation and emission slit widths were set at 8 nm and the polarizers to the magic angle conditions. As we wish to study carbazole excimers, the excitation wavelength was selected at 294 nm, where the benzyl groups of PS units hardly absorb. Absorbances at this wavelength were in the range 0.1–0.3. Solvent baselines were measured and subtracted from the fluorescence spectra. Preparation of polymers dilute solution in glassy PMMA was described elsewhere [26]. Right angle geometry, regular quartz 10 mm path cells and a temperature of 25 °C was used for measurements in dilute fluid solutions. For the solid samples of polymers, front-face illumination with the incident beam forming a 60° angle and room temperature were employed.

Table 1
Feed, copolymer composition of styrene and number average sequence length of monomers in copolymers

Sample	Mol fraction of styrene in feed, f_2	Mol fraction of styrene in copolymer, F_2	Number average sequence length of	
			VCz, $\bar{n}_1$	Styrene, $\bar{n}_2$
P0 (PVCz)	0.000	0.000	∞	0.00
P1	0.050	0.223	3.18	1.27
P2	0.365	0.807	1.20	3.90
P3	0.414	0.819	1.16	4.56
P4	0.574	0.831	1.08	7.80
P5	0.645	0.894	1.06	10.17
P6	0.742	0.962	1.04	15.51
P7	0.805	0.953	1.03	21.83
P8	0.900	0.980	1.01	46.41
P9	0.948	0.963	1.01	92.97
P10 (PS)	1.000	1.000	0.00	∞

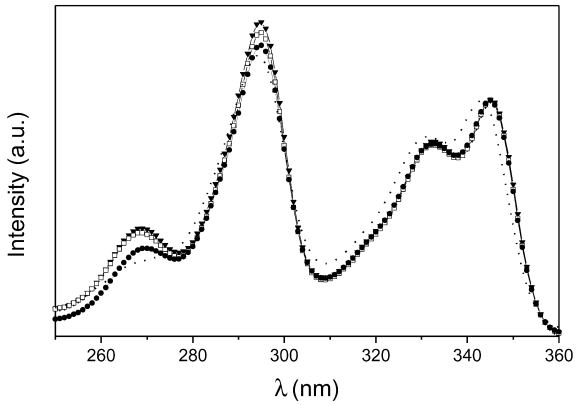

Fig. 4. Excitation spectra normalized at the peak of low energy 345 nm (343 nm for P0) for P0 (dashed curve) and the copolymers P3 (-■-), P5 (-□-) and P9 (-▼-) in dilute solution of DCM at 25 °C upon 375 nm.

The amount of intramolecular excimers for P# was obtained from the emission spectrum, by the I_E/I_M ratios, which were corrected by subtracting the fluorescence of the monomer at the excimer wavelength according to

$$I_E/I_M = (I_{P\#,\lambda_E} - I_{ECz,\lambda_E})/I_{M(norm)}, \quad (2)$$

where $I_{P\#,\lambda_E}$ is the normalized fluorescence intensity for P# at the wavelength of the excimer band, λ_E. I_{ECz,λ_E} is the normalized intensity obtained with the ECz model compound at λ_E and $I_{M(norm)}$ is the intensity at the monomer wavelength that is used for normalization of the emission spectra.

Fig. 4 depicts excitation spectra normalized at the peak of small energy 345 nm (343 nm for P0) for the copolymers P3, P5 and P9 and homopolymer P0 in dilute solution of DCM at 25 °C upon 375 nm. Excitation spectra of dilute solutions of other copolymers are very similar and they present features similar to the absorption spectra. Peaks for copolymers are observed at ~268, ~295, ~334, and ~345 nm. For P0, these maxima are slightly shifted to lower wavelengths. Intensities of peaks of highest energies (268 and 295 nm), where the benzyl group absorbs, increase with the PS content. Besides this, the spectra do not change significantly upon changing the emission wavelength.

Fig. 5 depicts emission spectra for fresh solutions of ECz and P# in DCM at 25 °C (left) and in the solid PMMA matrix at room temperature (right) upon 294 nm as excitation wavelength. Spectra are normalized at the maximum of the monomer emission band obtained for ECz in each solvent. This maximum, placed at ~350 nm, corresponds to the peak of higher energy of the ECz spectrum that also shows bands centered at ~365 nm and, a less pronounced one, at ~385 nm. In both figures the emission spectra for P0 and some copolymers, those with higher Cz content, show a broadening band toward the low energy zone of the monomer band observed for ECz. As the benzene groups from styrene units are not excited at 294 nm and as the spectroscopic properties of both Cz and Bz chromophores do not make the excitation energy transfer

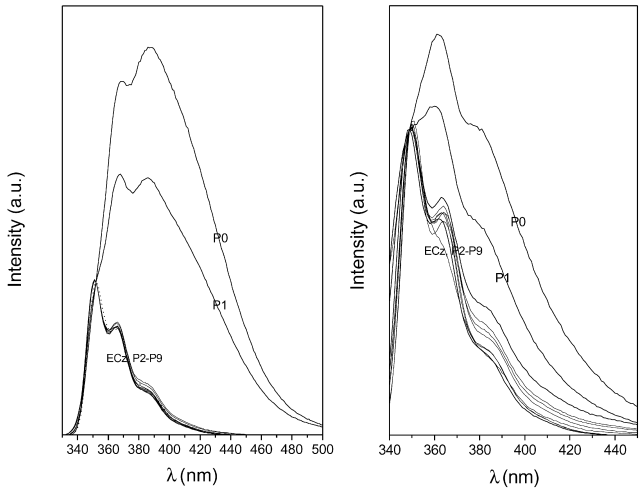

Fig. 5. Emission spectra for fresh solutions of ECz and P# in DCM at 25 °C (left) and in the solid PMMA matrix at room temperature (right) upon 294 nm as excitation wavelength. Spectra are normalized at the maximum of the monomer emission band obtained for ECz in each solvent.

from the Cz to Bz groups possible, this broadening is attributed to the Cz excimers. Although this is only noticeable for the first two members of the polymers studied, P0 and P1, the excimer emission intensity, as expected, seems to decrease monotonically with the molar ST content. According to Table 1, the first two members of the series, P0 and the copolymer P1, have an average number of Cz (ST) sequences $\bar{n}_1 \geq 3$ ($\bar{n}_2 \leq 1.3$) (or monomer Cz molar content >77%). P0 obviously has Cz–Cz···Cz sequences while P1 on average has Cz–Cz–Cz and Cz–$ST_{1.3}$–Cz sequences. The other components of the series P2–P9 have number average Cz (ST) sequences $\bar{n}_1 \leq 1.2$ ($\bar{n}_2 \geq 3.9$) (or monomer Cz molar content <20%). These polymers, which hardly show Cz–Cz sequences in the chain, exhibit emission characteristics very similar to a dilute solution of the model ECz. These results indicate that Cz–Cz sequences are probably responsible for most of the excimers. This was also found for copolymers poly(VCz-*co*-MMA) [21].

Placements of the maxima of excimer emission and relative intensities also depend on the nature of solvents used and on the time. Table 2 resumes the results of I_E/I_M for P# in fresh dilute solution of five dilute fluid solvents and in the solid PMMA matrix at the wavelengths of the low- and high-energy excimers. Besides the solvents used, copolymers with number average sequences of Cz (ST) such as $\bar{n}_1 \leq 1.2$ and $\bar{n}_2 \geq 3.9$ hardly shows excimers. This behavior is observed at the two different wavelengths. As the values of the number average sequences of Cz and MMA in poly(VCz-*co*-MMA) copolymer series studied previously by us [21] are not the same, it is not easy to compare the influence on the amount of excimers upon changing the monomer MMA by ST. However, for the poly(VCz-*co*-MMA) copolymers with number average sequences of Cz around 1 and of MMA between 2.7 and 3.6 the amount of excimer emission is noticeable. We can

Table 2
Experimental I_E/I_M corrected ratios for P# samples in dilute solution of different solvents measured at the wavelengths (λ_E) usually attributed to high and low energy excimers

Solvent	λ_E (nm)	Sample									
		P0	P1	P2	P3	P4	P5	P6	P7	P8	P9
THF[a]	375	2.07	1.75	0.02	0.01	0.01	0.00	0.00	0.00	0	0
	420	1.93	1.53	0.03	0.02	0.02	0.01	0.00	0.00	0	0
p-D[a]	375	1.83	1.13	0.00	0.00	0.00	0.00	0.00	0.00	0	0
	420	1.69	1.06	0.02	0.01	0.01	0.00	0.00	0.00	0	0
DCE[a]	375	2.71	1.69	0.00	0.00	0.00	0.00	0.00	0	0	0
	420	2.21	1.35	0.00	0.00	0.00	0.00	0.00	0.00	0.00	0
DCM[a]	375	1.86	1.29	0.04	0.02	0.00	0.00	0.00	0	0	0
	420	1.77	1.18	0.04	0.03	0.01	0.01	0.00	0.00	0	0
MMA[a]	375	0.77	0.45	0.02	0.00	0.00	0.00	0.00	0	0	0
	420	0.66	0.36	0.03	0.02	0.01	0.00	0.00	0	0	0
PMMA[b]	375	0.38	0.14	0.09	0.07	0.01	0.01	0.02	0.07	0.03	0
	420	0.14	0.08	0.05	0.04	0.01	0.01	0.00	0.00	0.00	0

[a] Measured in liquid state at 25 °C.
[b] Measured in solid the state at room temperature.

therefore predict that for similar number average sequences of monomer units, copolymers containing MMA units instead of ST ones can form more excimers. This is not surprising as the ST units contain a bulky benzyl group. Although for poly(VCz-*co*-MMA) the most important contribution to excimers was from Cz–Cz sequences, theoretical results also predicted the possibility of formation between Cz groups separated by one or even two MMA units [21].

As there are two polymers, P0 and P1, that really show excimer emission we only have two values with which to compare the I_E/I_M ratios measured in MMA fluid solution with those measured in the PMMA solid matrix. However, as should be expected, they show a decreasing in the amount of intramolecular excimer when increasing the medium rigidity. The presence of a rigid environment, where the chain dynamics is suppressed, slightly decreases the content of total intramolecular excimer formation.

To study the amount of excimer formation with the solvent power, fluorescence measurements on P# were performed in THF/MET mixtures. THF and MET are good and poor polystyrene solvents, respectively. Fig. 6 shows I_E/I_M corrected ratios (I_E at 375 nm) for P# vs. vol% of the THF in the solvent mixture. P0 and P1, the only polymers which really show excimers, exhibit an increase of I_E/I_M as the THF solvent content increases, which is noticeable up to a THF content of ~75 vol%, keeping I_E/I_M ratios constant from here to 100 vol% THF content. The poorer solvent should reduce the dimension of the styrene chains, thereby improving the Cz chromophore interaction. The opposite behavior for P0 and P1 reveal that the amount of excimer by interaction between chromophores separated by a large number of MMA monomer units should be neglected. The increase of I_E/I_M observed for P0 and P1 is probably due to the influence of the nature of MET and THF solvents on the Cz–Cz interaction from nearest neighbor VCz units. Something similar occurred when studying poly(VCz-*co*-MMA) series [21].

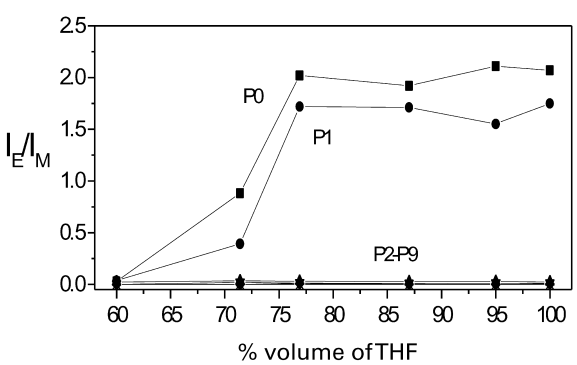

Fig. 6. Dependence of I_E/I_M at 375 nm on the vol% composition of mixtures THF/MET at 25 °C for P0 (-■-), P1 (-●-) and other copolymers.

3. Molecular dynamics

3.1. Methodology

The MD simulations were performed on (100%) isotactic and sindiotactic fragments containing three carbazole groups of the type CH_3–A–CH_2–B_n–A–CH_2–B_n–A–CH_3, where A = –CHCz–, B = –CHC_6H_5–CH_2– and $n = 0$–5. For simplicity they will be named I_n or S_n, respectively. An example of these structures is depicted in Fig. 7. For simulations, Sybyl 6.6 [27] with ground state parameters of Tripos Force Field [28] were used. Potential energy is the sum of bond stretching, angle bending, torsional, van der Waals, electrostatics and out-of-plane

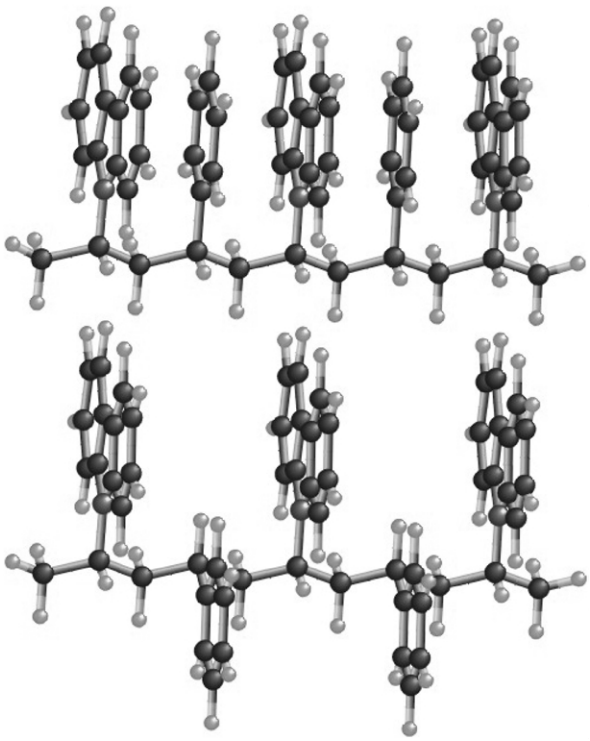

Fig. 7. Ball and stick structures of the fully extended conformations of the isotactic (I_1, top) and syndiotactic (S_1, bottom) fragments.

contributions. Charges were obtained by MOPAC (AM1) [29] for the all *trans* ECz and EBz structures. Charges and other geometric parameters are collected in Table 3. The simulations were started on minimized all *trans* conformations similar to the one depicted in Fig. 7 by using the simplex algorithm and the conjugate gradient (0.2 kcal/mol Å) as termination method [30,31]. Torsional ϕ_i bonds were defined using the standard procedure for vinyl polymers [32].

The simulations were of 1 ns, computed with a time step of 1 fs. Each simulation was started at 0 K, the temperature was increased by 10° at intervals of 300 fs up to reach the temperature of 600 K and then, the molecule was allowed to equilibrate at this temperature up to complete 100 ps. During the next 1 ns, the conformations were saved every 200 fs, giving $N = 5000$ conformations of each trajectory for later analysis. Velocities were rescaled at intervals of 10 fs. The high temperature of 600 K made it possible to avoid entrapments in conformational wells allowing a greater portion of conformational space to the sample during the relatively short trajectory.

As the only interest here were to study the carbazole excimers, each of the N pictures generated by MD, for each I_n or S_n fragment, were examined for fulfilling the conditions for the formation of a sandwich geometry for each pair of benzene (and pirrol) rings of adjacent and non-adjacent Cz group interactions. Possible adjustment in soft degrees of freedom, was taken into account by relatively relaxed excimer conformation criteria. These were

Table 3
Bond lengths, bond angles, and partial charges for the repetitive unit depicted in Fig. 1. Charges for hydrogen atoms (not tabulated) produce a neutral molecule

Bond	Length (Å)	Bond	Angle (°)	Atom[a]	Charges (esu)
$C1^{Cz}$–$C2^{Cz}$	1.540	$C1^{Cz}$–$C2^{Cz}$–$N3^{Cz}$	109.5	$C1^{Cz}$	0.125
$C2^{Cz}$–$N3^{Cz}$	1.450	$C2^{Cz}$–$N3^{Cz}$–$C4^{Cz}$	126.3	$C2^{Cz}$	0.126
$N3^{Cz}$–$C4^{Cz}$	1.348	$N3^{Cz}$–$C4^{Cz}$–$C5^{Cz}$	128.3	$N3^{Cz}$	−0.163
$C4^{Cz}$–$C5^{Cz}$	1.395	$C4^{Cz}$–$C5^{Cz}$–$C6^{Cz}$	117.2	$C4^{Cz}$	0.037
$C5^{Cz}$–$C6^{Cz}$	1.401	$C5^{Cz}$–$C6^{Cz}$–$C7^{Cz}$	121.8	$C5^{Cz}$	−0.173
$C6^{Cz}$–$C7^{Cz}$	1.404	$C6^{Cz}$–$C7^{Cz}$–$C8^{Cz}$	121.2	$C6^{Cz}$	−0.103
$C7^{Cz}$–$C8^{Cz}$	1.401	$C7^{Cz}$–$C8^{Cz}$–$C9^{Cz}$	117.4	$C7^{Cz}$	−0.173
$C8^{Cz}$–$C9^{Cz}$	1.395	$C8^{Cz}$–$C9^{Cz}$–$C4^{Cz}$	121.3	$C8^{Cz}$	−0.069
$C9^{Cz}$–$C10^{Cz}$	1.398	$C9^{Cz}$–$C4^{Cz}$–$N3^{Cz}$	110.2	$C9^{Cz}$	−0.095
$C9^{Cz}$–$C4^{Cz}$	1.392	$C4^{Cz}$–$C9^{Cz}$–$C10^{Cz}$	106.2	$C10^{Cz}$	−0.096
		$C8^{Cz}$–$C9^{Cz}$–$C10^{Cz}$	132.6	$C11^{Cz}$	−0.071
				$C12^{Cz}$	−0.167
				$C13^{Cz}$	−0.103
				$C14^{Cz}$	−0.039
$C1^{Bz}$–$C2^{Bz}$	1.540	$C1^{Bz}$–$C2^{Bz}$–$C3^{Bz}$	109.4	$C1^{Bz}$	0.125
$C2^{Bz}$–$C3^{Bz}$	1.525	$C2^{Bz}$–$C3^{Bz}$–$C4^{Bz}$	120.0	$C2^{Bz}$	0.038
$C3^{Bz}$–$C4^{Bz}$	1.394	$C3^{Bz}$–$C4^{Bz}$–$C5^{Bz}$	120.0	$C3^{Bz}$	−0.224
$C4^{Bz}$–$C5^{Bz}$	1.394	$C4^{Bz}$–$C5^{5Bz}$–$C6^{Bz}$	120.0	$C4^{Bz}$	−0.079
$C5^{Bz}$–$C6^{Bz}$	1.394	$C5^{Bz}$–$C6^{Bz}$–$C7^{Bz}$	120.0	$C5^{Bz}$	−0.161
				$C6^{Bz}$	−0.078
				$C7^{Bz}$	−0.167
				$C8^{Bz}$	−0.024

$3.35 < d_z < 3.9$ Å; $0 < d_{xy} < 1.35$ Å and $0 < \Psi < 40°$. d_z is the shortest of the distances between the center of mass of a benzene (or pirrol) ring in one Cz unit and the mean plane of a benzene (or pirrol) ring in another Cz unit and vice versa, d_{xy} is the lateral offset of the two benzene (or pirrol) rings that defines d_z, and Ψ is the angle between planes of the Cz groups that interact. The types of intramolecular face-to-face complexes formed, can be classified according to whether they produce a simultaneous overlap of the three rings for each pair of Cz groups or whether there is an overlap of one (or two) benzene or pirrol ring of one carbazole with one (or two) benzene or pirrol ring of the other carbazole unit.

The probability of the conformations which can adopt a sandwich geometry p_{tot} was evaluated as the fraction $p_{tot} = \frac{N_{exc}}{N}$, where N_{exc} is the number of conformations which satisfy the excimer requirements of the total conformations N. Intramolecular excimers by non-adjacent chromophores interaction ($p_{non\text{-}adj}$) were also distinguished from those formed by adjacent chromophore interaction (p_{adj}). In the last case, the probability was defined as $p_{adj} = p_{tot}(1 - p_{non\text{-}adj})$. The population of intramolecular excimers is considered proportional to p_{tot}. This method does not provide for the possibility of excimer population by dynamic, long-range interaction and energy transfer contributions.

Table 4 collects the results from the analysis of MD simulations on I_n and S_n trichromophoric compounds at

Table 4
Total probability for a face-to-face complex-forming conformation p_{tot}, the contributions due to interaction between adjacent (p_{adj}) and non-adjacent chromophores ($p_{non\text{-}adj}$) and the participation (%) of the different types of excimers by simultaneous interaction of one, two or three (benzene or pirrol) rings of each pair of Cz groups obtained from the analysis MD simulations on pure iso- (I_n) and sindiotactic (S_n) ($n = 0–5$) fragments at 600 K

Parameter	Fragment					
	I_0	I_1	I_2	I_3	I_4	I_5
p_{tot}	0.562	0.038	0.003	0.001	0.003	0.004
p_{adj}	0.556	0.038	0.003	0.001	0	0.004
% 1 ring	73.2	89.5	100.0	100	0	66.7
% 2 rings	21.0	7.8	0	0	0	33.3
% 3 rings	5.7	2.6	0	0	0	0
$p_{non\text{-}adj}$	0.005	0	0	0.000	0.003	0.000
% 1 ring	96	0	0	100	100	76.9
% 2 rings	0	0	0	0	0	15.4
% 3 rings	4	0	0	0	0	7.7
	S_0	S_1	S2	S_3	S_4	S_5
p_{tot}	0.461	0.221	0.003	0.001	0.002	0.001
p_{adj}	0.439	0.221	0.003	0.001	0.002	0
% 1 ring	83.9	91.9	100.0	100	80	0
% 2 rings	14.8	6.3	0	0	20	0
% 3 rings	1.3	1.8	0	0	0	0
$p_{non\text{-}adj}$	0.047	0	0	0	0	0.001
1 ring	89.0	0	0	0	0	100
2 rings	7.6	0	0	0	0	0
3 rings	3.4	0	0	0	0	0

600 K collecting the probability for a face-to-face complex-forming conformation by interaction between adjacent and non-adjacent Cz chromophores. Table 4 also shows the participation of the different excimers by simultaneous interaction of one, two or three rings of each pair of Cz groups. The fragments I_0 and S_0 obviously show the largest p_{tot}, this value being larger for I_0 than for S_0. The last statement agrees with the experimental evidence of several authors when studying PVCz [2] and dimeric model compounds [10,16,17]. The largest contribution to p_{tot} comes from the interaction between adjacent Cz. In fact the contribution due to interaction between non-adjacent Cz groups represents less than 1% of p_{tot} for I_0 and only ~10% for S_0. This fact also agrees with our experimental results and with the extended statement that most of the Cz excimers of PVCz are due to Cz–Cz nearest neighbor interactions [6,18,19]. Regarding the type of excimers by the amount of overlapping, most of them are partial, i.e. those which are responsible for the high-energy excimer. The number of conformations with total overlapping of Cz groups is considerably smaller. I_0 shows the largest number of conformations capable of potentially forming low energy excimers between adjacent Cz, ~159 conformations of ~2800 capable of forming excimers can satisfy the criteria for total overlapping. This number decreases for S_0, where

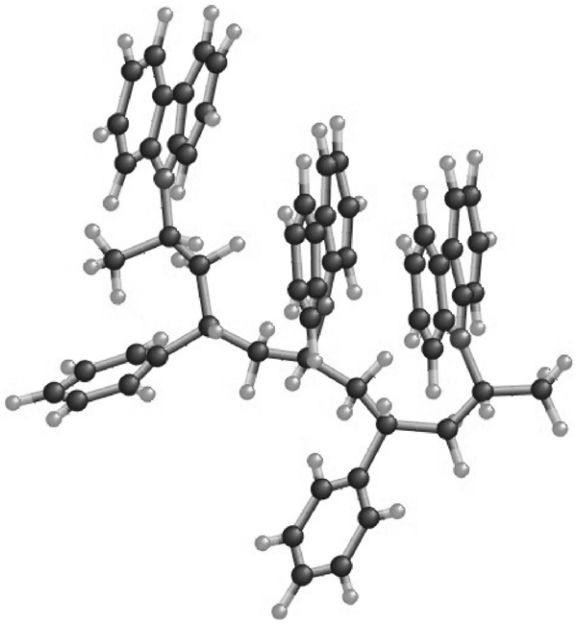

Fig. 8. A conformation of S_1 that fulfils the criteria of excimer by totally eclipsed interaction between a pair of adjacent Cz groups. The torsion angles of the main chain between this pair of Cz groups are 169, 99, −151.5 and −148.3°; the average of distance between Cz groups is 3.6 Å and $\Psi = 26°$.

out of ~2300 only 29 fulfill these requirements. Nevertheless, only 8 conformations of S_0 can form this type of excimers by interaction of non-adjacent Cz groups.

The value of p_{tot} seems to decrease with n. In fact, p_{tot} is only significant for $n \leq 1$. For $n > 1$ just a few conformations can reach the excimer geometry. I_1 and S_1, which show a noticeable probability for face-to-face complex forming between adjacent Cz, present a certain peculiarity, the syndiotactic form exhibits a larger value of p_{tot} than the isotactic one. This fact, which did not occur when studying similar fragments with MMA instead of ST [21], is also due to the presence of the bulky benzyl group of styrene units. These theoretical results qualitatively agree with the fact that only the P0 and P1 polymers exhibit intramolecular excimers. They also permit to reinforce that Cz–Cz sequences are almost totally responsible for the excimer formation in P0 and copolymers and that some Cz–ST–Cz, mainly syndiotactic, sequences could also slightly contribute to them. Fig. 8 depicts, as an example, a conformation of S_1 that fulfils the criteria of excimer by interaction between a pair of nearest neighbor carbazole groups.

4. Conclusions

Steady-state fluorescence emission spectra of dilute solutions for PVCz homopolymer and *N*-vinyl carbazole/styrene copolymers of different molar compositions upon only the excitation of carbazole chromophores, were obtained. Broadening to the red of monomer emission

indicates the presence of intramolecular excimers. However, the amount of excimers is only noticeable for the PVCz and the copolymer with the highest Cz content. These polymers have a number average of Cz (ST) sequences $\bar{n}_1 \geq 3$ ($\bar{n}_2 \leq 1.3$). Other copolymers having number average Cz (ST) sequences $\bar{n}_1 \leq 1.2$ ($\bar{n}_2 \geq 3.9$) do not exhibit intramolecular excimers. These results, which are also corroborated by MD, point out that most of intramolecular excimers are due to Cz–Cz sequences in the chain. Nevertheless, some Cz–ST–Cz, mainly syndiotactic, sequences could also slightly contribute to the excimer population. MD analysis also demonstrates the experimental evidence that isotactic fragments of Cz–Cz sequences gives a larger amount of excimer conformations than sindiotactic ones. Due to the high concentration of chromophores and the relatively low amount of excimers, the poly(VCz-*co*-ST) copolymers could be potentially interesting from the photoconduction viewpoint. The study of the excitation energy transfer will be the objective of another work.

Acknowledgements

This research was supported by MCYT BQU2001-1158. We express thanks to M.L. Heijnen for assistance with preparation of the manuscript.

References

[1] Solaro R, Galli G, Ledwit A, Chiellini E. In: Phillips D, editor. Polymer photophysics: luminescence, energy migration and molecular motion in synthetic polymers. New York: Chapman & Hall; 1985. p. 377.
[2] Itaya K, Okamoto K, Kusabayashi S. Bull Chem Soc Jpn 1976;49: 2082.
[3] Klöpffer W. Chem Phys Lett 1969;4:193.
[4] Johnson PC, Offen HW. J Chem Phys 1971;55:2945.
[5] Johnson GE. J Chem Phys 1975;62:4697.
[6] Yokoyama M, Tamamura T, Atsumi M, Yopshimura M, Shirota Y, Mikawa H. Macromolecules 1975;8:101.
[7] Venokonas GW, Powell RC. Chem Phys Lett 1975;34:601.
[8] Hoyle CE, Nemzek TL, Mar A, Guillet JE. Macromolecules 1978;11: 429.
[9] De Schryver FC, Demeyer K, van der Auweraer M, Quanten E. Ann NY Acad Sci 1981;366:93.
[10] De Schryver FC, Vandendriessche J, Toppet S, Demeyer K, Boens N. Macromolecules 1982;15:406.
[11] Masuhara H, Tamai N, Mataga N, De Schryver FC, Vandendriessche J. J Am Chem Soc 1983;105:7256.
[12] Vandendriessche J, Palmans P, Toppet S, Boens N, De Schryver FC, Masuhara H. J Am Chem Soc 1984;106:8057.
[13] De Schryver FC, Vandendriessche J, Demeyer K, Collart P, Boens N. Polym Photochem 1985;6:215.
[14] Vandendriessche J, De Schryver FC. Polym Photochem 1986;7:153.
[15] De Schryver FC, Collart P, Vandendriessche J, Goedeweeck R, Swinnen A, van der Auweraer M. Acc Chem Res 1987;20:159.
[16] Ito S, Takami K, Yamamoto M. Makromol Chem, Rapid Commun 1989;10:790.
[17] Ito S, Takami K, Tsujii Y, Yamamoto M. Macromolecules 1990;23: 2666.
[18] Skilton PF, Sakurovs R, Ghiggino KP. Polym Photochem 1982;2:409.
[19] Chiellini E, Solaro R, Galli G, Ledwith A. Macromolecules 1980;13: 1654.
[20] Davinson K, Soutar I, Swanson L, Yin J. J Polym Sci, Polym Phys Ed 1997;35:963.
[21] Gallego J, Pérez-Foullerat D, Mendicuti F, Mattice WL. J Polym Sci, Polym Phys Ed 2001;39:1272.
[22] Mattice WL, Suter UW. Conformational theory of large molecules. The rotational isomeric state model in macromolecular systems. New York: Wiley; 1994.
[23] Haile JM. Molecular dynamics simulation: elementary methods. New York: Wiley; 1992.
[24] Fineman M, Ross SD. J Polym Sci 1950;5:259.
[25] Kelen T, Tüdos F. J Macromol Sci-Chem 1975;A9(1):1.
[26] Mendicuti F, Saiz E, Mattice WL. Polymer 1992;33:4908.
[27] Sybyl 6.6. St Louis, MO: Tripos Associates.
[28] Clark M, Cramer III RC, van Opdenbosch NJ. Comput Chem 1989; 10:982.
[29] MOPAC (AM1). Included in the Sybyl 6.6.
[30] Brunel Y, Faucher H, Gagnaire D, Rasat A. Tetrahedron 1975;31: 1075.
[31] Press WH, Flannery BP, Teukolski SA, Vetterling WT. Numerical recipes: the art of scientific computing. New York: Cambridge University Press; 1988. p. 312.
[32] Riande E, Saiz E. Dipole moments and birrefringence of polymers. Englewood Cliffs, NJ: Prentice-Hall; 1992.